Modifying Nobili-Durand surface energy for conically degenerate anchorings at the interface of liquid crystal colloids

Seyed Reza Seyednejad,[1] Takeaki Araki,[2] and Mohammad Reza Mozaffari[3,*]
[1]*Department of Physics, Institute for Advanced Studies in Basic Sciences (IASBS), Zanjan 45137-66731, Iran*
[2]*Department of Physics, Kyoto University, Sakyo-ku, Kyoto 606-8502, Japan*
[3]*Department of Physics, University of Qom, Qom 3716146611, Iran*

(Received 9 January 2019; published 11 March 2019)

We propose a surface energy for conically degenerate anchorings of uniaxial liquid crystal mesogens by modifying tensorial Nobili-Durand surface energy that is usually employed for fixed anchoring orientations with preferred polar angles. By minimizing Landau–de Gennes free energy and the proposed surface energy, we obtain the equilibrium director configuration around a spherical colloid in the uniform nematic liquid crystal. Our calculations show that the proposed surface energy can cause boojum or/and Saturn-ring defect textures depending on the equilibrium conic angle. We also study the interactions between two spherical colloids with the equilibrium conic angle 45°, where the surface energy provides both boojum and Saturn-ring defects on the surface of particles. We compare the calculated anisotropic colloidal interactions with experimental observations [B. Senyuk *et al.*, Nat. Commun. **7**, 10659 (2016)]. In agreement with experiment, our results show two stable angular assemblies in the close particle-particle separations. Also, the long-range elastic interactions are almost consistent with the hexadecapolar elastic distortion.

DOI: 10.1103/PhysRevE.99.032702

I. INTRODUCTION

Behavior of colloidal particles in a nematic liquid crystal (NLC) host is controlled not only by the size and shape of the particles [1–5] but also by the anchoring alignment and strength of the liquid crystal mesogens on the particle surface [6–10]. There are a wide range of studies on micro- and nanospherical colloids with planar or normal anchorings in a uniform NLC [11–17]. The uniform alignment of the nematic orientation (i.e., director) gets perturbed by the anchoring on the surface of the particles, and then spatial discontinuities of the director field are often formed around the particles as points and/or lines. These discontinuities, known as topological defects, are strongly related to long- and short-range colloidal interactions in the NLC host [18].At large distances, the colloid and its accompanying defect act as a multipole elastic moment in analogy to those in the electrostatics [10,19–24]. The interaction between the particles can be approximated by that between the multipole moments. In short particle-particle distances, on the other hand, we sometimes observe that the defect textures rearrange at the particle contact faces because of the symmetry breaking of the director field [6,7]. The balance between the long- and the short-range interactions can provide colloidal self-assemblies [2,9]. The anisotropic elastic interactions between the colloids in the close distances overcome the Brownian motion and enable regular one- or two-dimensional stable structures to form [14].

In contrast to the spherical colloids, faceted colloids build up more complex structures because of the defect line deformations at the sharp edges [3,4,25–28]. Although colloids with low symmetry open a new route for the colloidal self-assembly with specific media elastic distortions, it has shown that the spherical colloids with various anchoring alignments can be still major candidates in scientific and technological studies on colloids [8–10].

The surface functionalization of the spherical colloids with different anchoring properties can induce complex elastic distortions and lead to the surface and the bulk defect textures simultaneously in the uniform NLC. Such particles that have specific surface properties are known as Janus colloids [8]. They can potentially form novel colloidal structures in comparison to particles with fully planar or normal colloidal anchorings. Another interesting idea for inducing complex elastic deformations around the spherical colloids has been recently studied by Senyuk and his coworkers. They imposed a conically degenerate boundary condition on the director at the colloidal surfaces. In the uniform NLC fluid, these particles induce hexadecapolar director distortions that causes anisotropic colloidal interactions. Depending on the study conditions, the colloidal interactions can spatially form two-dimensional regular crystals with rhombic unit cells or any possible three-dimensional lattices [9]. A particle with the hexadecapolar symmetry behaves as a 16-pole moment in analogy to those in the electrostatics.A specific distribution of charges on a spherical particle corresponds to a filled g orbital of the outermost occupied electron shells of chemical elements [9,10].

The colloids immersed in the NLC is described by appropriate surface energies that satisfy the nematic mesogens orientations on the surface of the particles [29–33]. The normal and planar anchoring surfaces have been usually employed in studying the nematic colloids. To investigate the colloids with complex anchorings such as the conically degenerated

*m.mozaffari@qom.ac.ir

anchoring theoretically, we need new proper surface energies. It is quite useful to describe the surface energies with a tensorial form, because it can describe the director field around the defects without considering singularities [30,31,33]. To consider a nondegenerate and fixed anchoring condition, a tensorial quadratic surface energy was introduced by Nobili and Durand (ND) [30]. Another tensorial surface energy has been proposed by Sluckin and Poniewierski (SP) for preferred orientations [31]. Fournier and Galatola (FG) also proposed a smart surface energy for the degenerate planar anchoring [33].

In this study, we modify the ND surface energy to describe the conically degenerate anchorings of the uniaxial NLC. We mathematically compare the modified ND and the SP surface energy behaviors around the equilibrium conic angle by evaluating their reduced nontensorial energies. By minimizing the Landau–de Gennes free energy with the surface energies, we consider the director arrangement on a spherical colloid in the uniform NLC for different equilibrium conic angles. We also explain interactions between two colloids with the modified ND surface energy with the equilibrium conic angle 45° and compare the results with experimental observations [9].

II. SURFACE ENERGY

To describe a nematic fluid, we use a traceless and symmetric tensor order parameter, Q_{ij}. In a uniaxial nematic fluid, it is given as $Q_{ij}(\vec{r}) = S(\vec{r})\{3\hat{n}_i(\vec{r})\hat{n}_j(\vec{r}) - \delta_{ij}\}/2$, where S is the scalar order parameter and $\hat{n}$ is the unit vector along the director orientation. The anchoring energy of the NLC molecules on the colloid surface is usually given as $\mathcal{F}_S = \int_{\partial\Omega} f_S d\mathcal{S}$, in which $\int_{\partial\Omega} d\mathcal{S}$ denotes the integral over the colloid surfaces and f_S is a function of Q_{ij}. Here the anchoring strength W appears as a coefficient in the surface energy density. In this study, the surface scalar order parameter is assumed to be the same with that in the bulk, S_b (see below). A degenerate conical anchoring can potentially include all anchoring situations from the normal to the degenerate planar anchorings, depending on the equilibrium conic angle, ψ_e.

Sluckin and Poniewierski (SP) have proposed a general form of the surface energy as

$$f_S^{\mathrm{SP}} = c_1\hat{\nu}_i Q_{ij}\hat{\nu}_j + c_2 Q_{ij}Q_{ji} + c_3\hat{\nu}_i Q_{ik}Q_{kj}\hat{\nu}_j + c_4(\nu_i Q_{ij}\nu_j)^2, \tag{1}$$

where $\hat{\nu}$ is the unit normal vector of the surface, and c_1, c_2, c_3, and c_4 are material constants [31]. The indices (i, j, k) refer to Cartesian coordinates, and Einstein summation convention is assumed. Here we retain only the first and the last terms and ignore the others. In this specific case, the SP surface energy is rewritten as

$$\tilde{f}_S^{\mathrm{SP}} = W\{\hat{\nu}_i Q_{ij}\hat{\nu}_j - S_b P_2(\cos\psi_e)\}^2, \tag{2}$$

where $P_2(x)$ is the second-order Legendre polynomial function of x. It can describe the conically degenerate anchoring of the uniaxial nematic liquid crystal. This SP surface energy density reduces to a nontensorial conical anchoring energy as

$$\tilde{f}_S^{\mathrm{SP}} = W\left(\frac{3S_b}{2}\right)^2 \sin^2(\psi + \psi_e)\sin^2(\psi - \psi_e), \tag{3}$$

where $\hat{n}\cdot\hat{\nu} = \cos\psi$ and $\hat{n}_e\cdot\hat{\nu} = \cos\psi_e$ (see Fig. 1). This nontensorial form was also given by Ramdane *et al.* [32].

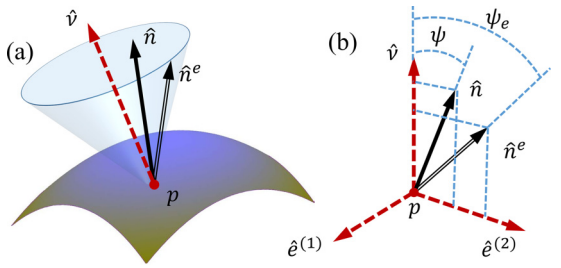

FIG. 1. (a) A schematic picture of the normal unit vector $\hat{\nu}$ and nematic director orientation $\hat{n}$ on the local surface. $\hat{n}^e$ is the equilibrium conical orientation. (b) A local right-handed coordinate system to characterize equilibrium conical orientation, $\hat{n}^e$. It is defined by the three unit vectors, $\hat{e}^{(1)}$, $\hat{e}^{(2)}$ and $\hat{\nu}[=\hat{e}^{(1)}\times\hat{e}^{(2)}]$. ψ_e is the equilibrium conic angle with respect to the normal unit vector [9].

Around its minimum, $\psi = \psi_e$, it is mathematically approximated as

$$\tilde{f}_S^{\mathrm{SP}} \simeq W(3S_b/2)^2\{\sin^2(2\psi_e)(\psi-\psi_e)^2 + \sin(4\psi_e)(\psi-\psi_e)^3 + (7\cos(4\psi_e) - 1)(\psi - \psi_e)^4 + \cdots\}. \tag{4}$$

In this Taylor expansion, the coefficient of the quadratic term, which evaluates the effective anchoring strength, is given by $W(3S_b/2)^2\sin^2(2\psi_e)$. This indicates that the effective anchoring strength depends on ψ_e and, in particular, vanishes for the normal ($\psi_e = 0°$) and the fully planar ($\psi_e = 90°$) anchoring conditions. When $\psi_e = 0°$ and $\psi_e = 90°$, the fourth order term becomes dominant.

To resolve this difficulty, we propose another surface energy in a tensorial form by modifying the ND surface energy scheme [30]. It is given by

$$f_S^{\mathrm{mND}} = \frac{W}{2}(Q_{ij} - Q^e_{ij})(Q_{ji} - Q^e_{ji}). \tag{5}$$

In this modified Nobil-Durand (mND) model, as shown in Fig. 1(a), $Q^e_{ij} = S_b(3\hat{n}^e_i\hat{n}^e_j - \delta_{ij})/2$ is locally determined by the equilibrium conical orientation, $\hat{n}^e$, on the surface. The equilibrium conical orientation can freely rotate azimuthally around the normal unit vector, $\hat{\nu}$. As shown in Fig. 1(b), the equilibrium conical orientation is defined by

$$\hat{n}^e = \hat{\nu}\cos\psi_e + \hat{e}^{(2)}\sin\psi_e, \tag{6}$$

where $\hat{e}^{(2)} = \hat{\nu}\times\hat{e}^{(1)}$. $\hat{e}^{(1)}$ is a unit vector perpendicular to the plane containing $\hat{n}$ and $\hat{\nu}$. In order to preserve the nematic symmetry, it is given by $\hat{e}^{(1)} = (\hat{u}\times\hat{\nu})/|\hat{u}\times\hat{\nu}|$, where $\hat{u}$ is given by $\hat{u} = \hat{n}$ when $\hat{n}\cdot\hat{\nu} \geqslant 0$ or $\hat{u} = -\hat{n}$ otherwise. To avoid a singularity in obtaining $\hat{e}^{(1)}$ when $\hat{\nu}\times\hat{n} = 0$ in numerical minimizations, we add random noises in the initial director so that $\hat{\nu}\times\hat{n} \neq 0$. In contrast to the original quadratic ND surface energy, in which the equilibrium nematic tensor Q^e is fixed, the mND surface energy is nonquadratic potential because the equilibrium tensor depends on the local tensor.

In the director notation, the mND surface density reduces to the Rapini-Papoular (RP) surface density [29] as

$$f_S^{\mathrm{RP}} = W\left(\frac{3S_b}{2}\right)^2\{1 - (\hat{n}\cdot\hat{n}^e)^2\} = W\left(\frac{3S_b}{2}\right)^2\sin^2(\psi - \psi_e), \tag{7}$$

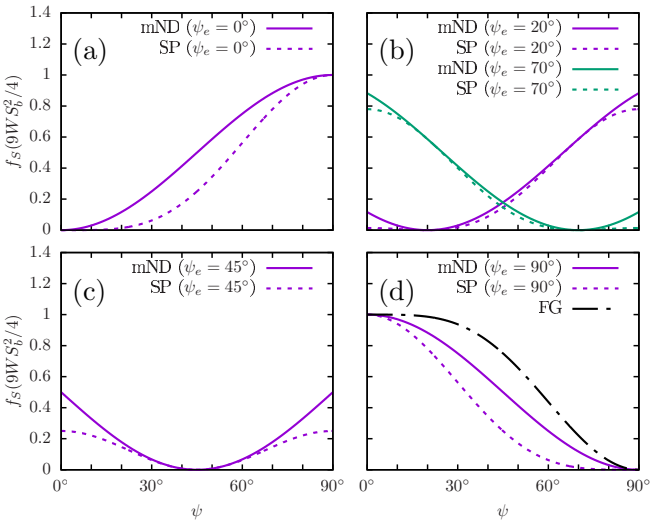

FIG. 2. Plots of the modified Nobili-Durand and Sluckin-Poniewierski surface energies for the generate anchorings (a) $\psi_e = 0°$ (normal), (b) $\psi_e = 20°$ and $70°$, (c) $\psi_e = 45°$, and (d) $\psi_e = 90°$ (planar). In (d), the Fournier-Galatola surface energy is also shown.

where $\hat{n} \cdot \hat{n}^e = \cos(\psi - \psi_e)$. This form has been used to study the nematic droplets with the conical anchoring [34]. The RP surface anchoring behaves around its minimum as $f_S^{\mathrm{RP}} \simeq W(3S_b/2)^2[(\psi - \psi_e)^2 - (\psi - \psi_e)^4/3 + \cdots]$. Around the minimum, the anchoring strength is effectively given as $W(3S_b/2)^2$, which is independent of ψ_e, in contrast to the SP surface energy. Equation (5) is applicable for any conic angles, $0° < \psi_e \leqslant 90°$. For $\psi_e = 0°$, it describes the standard ND approach for the perpendicular anchoring as $Q_{ij}^e = S_b(3\hat{\nu}_i\hat{\nu}_j - \delta_{ij})/2$. On the other hand, it gives the degenerate planar anchoring as $Q_{ij}^e = S_b[3\hat{e}_i^{(2)}\hat{e}_j^{(2)} - \delta_{ij}]/2$ when $\psi_e = 90°$.

Fournier and Galatola [33] also proposed another surface energy with the degenerate planar anchoring in the Landau–de Gennes form. Depending on the anchoring strength, W, the surface energy enforces the nematic mesogens to lie down on the surface along their projections. The surface energy density can be expressed as

$$f_S^{\mathrm{FG}} = W(\tilde{Q}_{ij} - \tilde{Q}_{ij}^{\perp})(\tilde{Q}_{ji} - \tilde{Q}_{ji}^{\perp}), \tag{8}$$

where $\tilde{Q}_{ij} = (3S_b/2)\hat{n}_i\hat{n}_j$ and $\tilde{Q}_{ij}^{\perp} = (\delta_{ik} - \hat{\nu}_i\hat{\nu}_k)\tilde{Q}_{kl}(\delta_{lj} - \hat{\nu}_l\hat{\nu}_j)$ are uniaxial parallel and projection tensors, respectively. The FG surface energy density is simplified with ψ as

$$f_S^{\mathrm{FG}} = W\left(\frac{3S_b}{2}\right)^2(1 + \sin^2\psi)\sin^2\left(\psi - \frac{\pi}{2}\right). \tag{9}$$

For a better insight, we compare the mND surface energy density [Eq. (7)] with the SP surface energy density [Eq. (3)] at different equilibrium conic angles, ψ_e. As shown in Fig. 2, the mND surface anchoring is more concave around $\psi = \psi_e$ in comparison with the SP surface anchoring. In Figs. 2(b) and 2(c), the mND surface anchoring has cusps $\psi = 0°$ and $90°$, where the derivative of the energy changes discontinuously. Both surface anchorings show the good agreement with each other when $\psi_e = 45°$. Also we compared the FG surface energy density [Eq. (9)] with the mND and SP surface energy densities at $\psi_e = 90°$. Figure 2(d) displays that the FG surface anchoring has a steeper slope around the minimum for the same anchoring strength, W.

III. NUMERICAL METHOD

In order to obtain the director field in the whole system, we minimize the total free energy $\mathcal{F} = \mathcal{F}_{\mathrm{LdG}} + \mathcal{F}_S$ numerically. $\mathcal{F}_{\mathrm{LdG}}$ is the Landau–de Gennes free energy of the bulk NLC and is given in terms of the tensor order parameter and its spatial derivatives as

$$\mathcal{F}_{\mathrm{LdG}} = \int_\Omega d\mathcal{V}\left(\frac{a_0\Delta T}{2}Q_{ij}Q_{ji} - \frac{B}{3}Q_{ij}Q_{jk}Q_{ki} + \frac{C}{4}(Q_{ij}Q_{ji})^2 + \frac{L_1}{2}\partial_k Q_{ij}\partial_k Q_{ij}\right), \tag{10}$$

where $\int_\Omega d\mathcal{V}$ is the integral over the volume occupied by the nematic liquid crystal in the cell [35]. The first three terms describe the isotropic-nematic phase transition. The coefficients a_0, B, and C are positive and material-dependent parameters, and $\Delta T = T - T^*$, where T^* is the nematic supercooling temperature. The bulk scalar order parameter in the uniform nematic phase is given by $S_b = (B/6C)(1 + \sqrt{1 - 24a_0\Delta T\, C/B^2})$. The last term is the contribution of elastic distortions in one-constant approximation. L_1 is its coefficient. With L_1 and S_b, the Frank elastic moduli are calculated as $K_{\mathrm{splay}} = K_{\mathrm{twist}} = K_{\mathrm{bend}} = 9L_1S_b^2/2$. We use the parameters of nematic liquid crystal 5CB ($a_0 = 0.087 \times 10^6$ J/m^3 K, $T^* = 307.15$ K, $T = 305.17$ K, $B = 2.12 \times 10^6$ J/m^3, $C = 1.73 \times 10^6$ J/m^3, $L_1 = 4 \times 10^{-11}$ J/m) [21,36]. The anchoring strength is assumed to be sufficiently large as $W = 10^{-2}$ J/m^2.

We study identical spherical colloids ($R = 0.5$ μm) in a cubic cell filled by the NLC ($L_x = L_y = L_z = 20R$). The director orientations on the cell walls are set along the z axis, $\hat{n}_0 = (0, 0, 1)$. The center of particles are spatially placed in the middle of cell and are restricted to the plane $y = L_y/2$. Numerically a finite-element method [17] is employed to minimize the total free energy ($\mathcal{F} = \mathcal{F}_{\mathrm{LdG}} + \mathcal{F}_S$). Using an automatic mesh generator Gmsh [37], the calculation domain decomposes into tetrahedral elements. The tensor order parameter elements are linearly interpolated within each mesh element. The validity of the linear interpolation depends on the order parameter deviations within each element, which is controlled by the mesh size. The Delaunay triangulation-tetrahedralization algorithm supplies the element size on the particle surfaces with $L_e = 0.01R$, and those on the cell boundaries with $L_e = R$. A conjugate gradient method [38] is used to minimize the free energy and the iteration steps are stopped when the free-energy difference between two sequential steps drops below 10^{-10}.

IV. NUMERICAL RESULTS

A. Director field around a single particle

Figure 3 shows the director orientations and defect structures around a spherical colloid with the degenerate conical anchoring on the surface for various values of the equilibrium

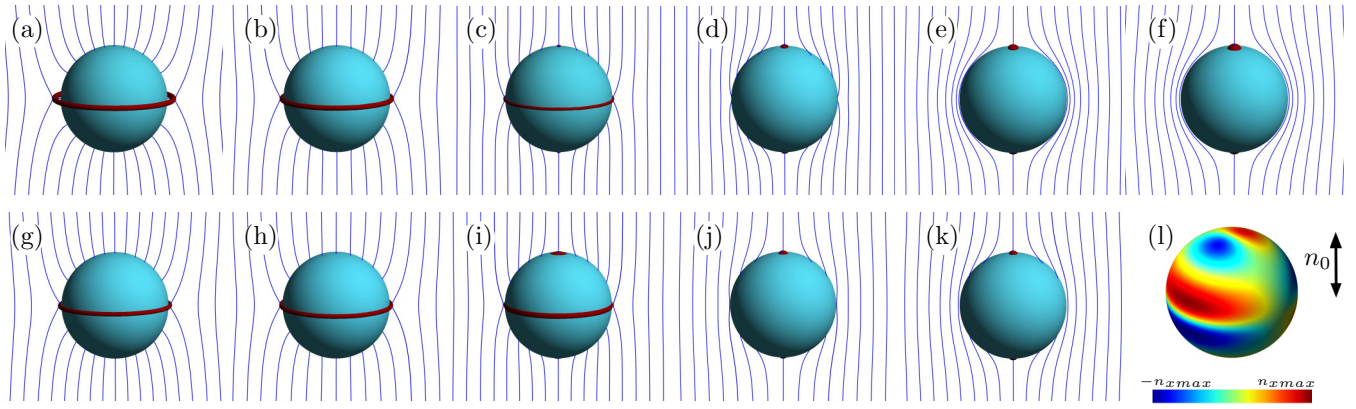

FIG. 3. Director orientations and defect structures around a spherical colloid in a uniform nematic media. The structures in (a)–(e) are obtained with the modified Nobili-Durand surface anchoring for various values of the equilibrium conic angle, (a) $\psi_e = 0^\circ$, (b) $\psi_e = 20^\circ$, (c) $\psi_e = 45^\circ$, (d) $\psi_e = 70^\circ$, and (e) $\psi_e = 90^\circ$. The pattern in (f) is related to the Fournier-Galatola surface anchoring calculation. Those in (g)–(k) are determined by the Sluckin-Poniewierski surface anchoring for various values of the equilibrium conic angle, (g) $\psi_e = 0^\circ$, (h) $\psi_e = 20^\circ$, (i) $\psi_e = 45^\circ$, (j) $\psi_e = 70^\circ$, and (k) $\psi_e = 90^\circ$. The anchoring constant is the same amount in all configurations ($W = 10^{-2}$ J/m^2). The regions, in which the scalar order parameter is lower than $0.5S_b$, are indicated by the red surfaces. They represent the defects of the director field. (l) A three-dimensional map plot of the x component of director, $\hat{n}_x$, on virtual spherical surface with radius $r = 1.2R$. The mND surface anchoring with $\psi_e = 45^\circ$ is employed. The maximum of $\hat{n}_x$ is 0.2.

conic angle, ψ_e, in a uniform nematic media. The director orientations in Figs. 3(a)–3(e) are obtained with the mND surface energy [Eq. (5)]. The red tubes represent the topological defects of the director field. They are defined by the regions, in which the scalar order parameter is lower than $0.5S_b$. Figure 3(a) refers to the normal anchoring ($\psi_e = 0^\circ$) which induces a Saturn-ring defect with the topological strength $s = -1/2$. An increase in ψ_e ($\leqslant 45^\circ$) shrinks the Saturn-ring defect loop. Finally the Saturn ring disappears from the bulk and a surface defect loop is formed. A further increase in ψ_e ($\geqslant 45^\circ$) leads to two surface point defects (boojums), which appear gradually at the poles in the nematic direction. Figure 3(e) represents the two boojums with the topological strength $s = +1$ for the perfect planar anchoring ($\psi_e = 90^\circ$). The director structure in Fig. 3(f) is obtained with the FG surface anchoring [Eq. (8)]. We confirmed that the mND surface energy gives the same result as that with the FG when $\psi_e = 90^\circ$ [see Figs. 3(e) and 3(f)]. For $\psi_e = 45^\circ$, both boojums and Saturn-ring defects are observed. This director and defect structure are consistent with those in the previous study with the experimental realizations [9]. It was claimed that this structure has a hexadecapole symmetry.

Figures 3(g)–3(k) show the director patterns with the SP surface energy [Eq. (3)]. Here the effective anchoring strength depends on ψ_e, contrary to the mND surface anchoring. Although the SP surface anchoring shows nearly similar results with those with the mND surface energy, some qualitative differences between them are found. In $\psi_e = 0^\circ$, the Saturn ring calculated with the SP surface energy is closer to the surface than that with the mND surface energy. In $\psi_e = 70^\circ$, the director deviations from the preferred orientation on the surface are not bound to the equator. In $\psi_e = 90^\circ$, the director cannot lie very well on the surface. We show the $\hat{n}$ profile in x direction around the particle with the mND anchoring with $\psi_e = 45^\circ$ at the radius $r = 1.2R$ in Fig. 3(l). The director distortions at $\psi_e = 45^\circ$ indicate a hexadecapolar symmetry (16-pole moment) similar with the filled g orbital of the outermost occupied electron shells of chemical elements [9,10].

In order to evaluate the local director alignment on the surface with respect to the equilibrium conical orientation, we introduce *anchoring error* quantity as $e_A = |(\hat{n} \cdot \hat{v})^2 - \cos^2 \psi_e|$. It gives the efficiency of the surface energies in different equilibrium conic angles. Figure 4 shows e_A patterns on the particle surface for the mND [Figs. 4(a)–4(e)], FG [Fig. 4(f)], and SP [Figs. 4(g)–4(k)] surface energies. Generally, the anchoring errors of the mND surface energy in Figs. 4(a)–4(e) are smaller than those of the SP surface energy in Figs. 4(g)–4(k). For $\psi_e = 90^\circ$, the mND surface anchoring gives almost the same configuration as that of the FG surface anchoring [see Figs. 4(e) and 4(f)]. The anchoring error of the SP energy becomes largest when $\psi_e = 45^\circ$. With a large anchoring strength, $W = 1$ J/m^2 and $\psi_e = 45^\circ$ [see Fig. 4(l)], the error can be diminished, but it is still larger than that of the mND energy in Fig. 4(c).

B. Interparticle interactions for $\psi_e = 45^\circ$

Next we investigate interactions between the two spherical colloids in the uniform nematic host. The colloids have the conically degenerate anchoring on their surfaces with the equilibrium conic angle $\psi_e = 45^\circ$. This setup aims at explaining recent experimental observations with similar conditions [9]. Here we employ only the mND surface energy to describe the conically degenerate anchoring. We should note that although the mND surface energy provides stronger anchoring on the surfaces, the mND and SP surface energies approximately exhibit almost the same behaviors when $\psi_e = 45^\circ$. The study on colloidal interactions with the SP energy will remain open.

In Fig. 5, we plot the interaction between the two particles as functions of the interparticle distance, D, and the angle between the line joining the center of particles and the far-field director, θ. To clarify the nature of the short-range

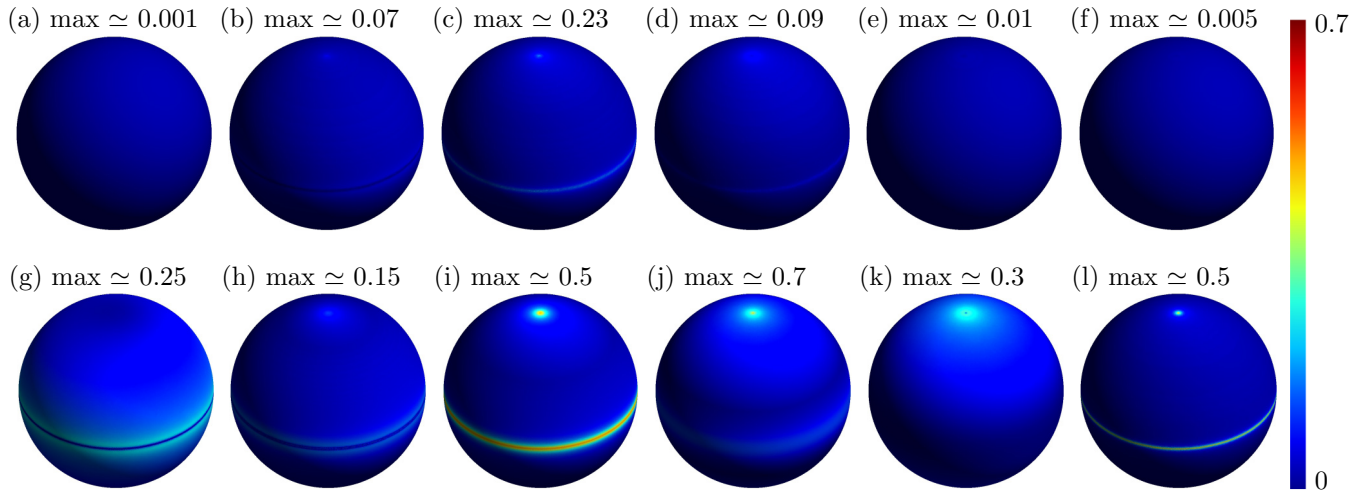

FIG. 4. Anchoring error patterns, e_A, on the colloid surface. The patterns in (a)–(e) are obtained with the mND surface energy for various values of the equilibrium conic angle, (a) $\psi_e = 0°$, (b) $\psi_e = 20°$, (c) $\psi_e = 45°$, (d) $\psi_e = 70°$, and (e) $\psi_e = 90°$. The pattern in (f) is related to the FG surface energy calculation. The patterns in (g)–(k) are determined by the SP surface energy for (g) $\psi_e = 0°$, (h) $\psi_e = 20°$, (i) $\psi_e = 45°$, (j) $\psi_e = 70°$, and (k) $\psi_e = 90°$. The anchoring constants are the same in (a)–(k) configurations ($W = 10^{-2}$ J/m^2). The pattern in (l) is obtained by the SP surface energy with $W = 1$ J/m^2 and $\psi_e = 45°$. The maximum values of e_A are indicated above the snapshots.

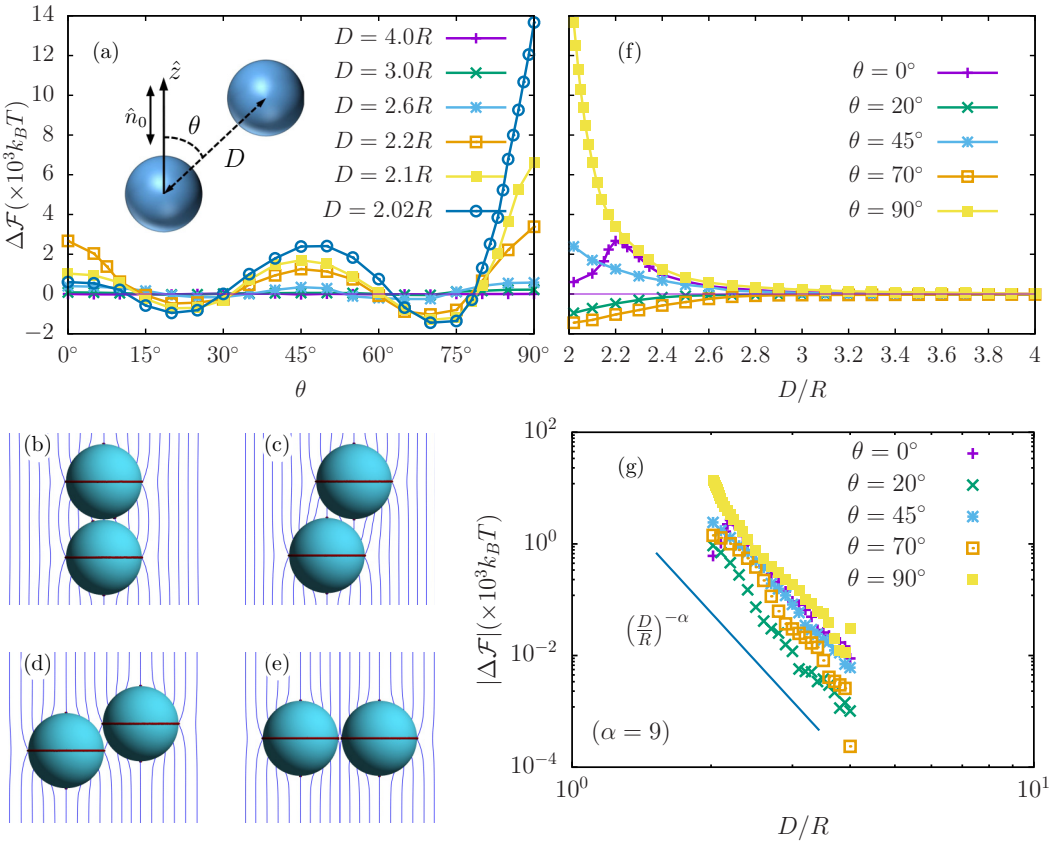

FIG. 5. Colloidal interactions in a uniform nematic media with the conical anchoring, $\psi_e = 45°$. (a) The angular dependence of the effective potential $\Delta\mathcal{F}$ for various fixed short and large distances, where $\Delta\mathcal{F} \equiv \mathcal{F} - \mathcal{F}_0$ and $\mathcal{F}_0 = \mathcal{F}(D = 4R) = 1.323 \times 10^5 k_B T$. The inset plot displays a schematic of spatial arrangement of spherical particles with respect to the far-field director orientation, $\hat{n}_0$. [(b)–(e)] The equilibrium profiles of the director field and scalar order parameter in close contacts for (b) $\theta = 0°$ and $D/R = 2.02$, (c) $\theta = 20°$ and $D/R = 2.10$, (d) $\theta = 70°$ and $D/R = 2.10$, and (e) $\theta = 90°$ and $D/R = 2.02$. The regions, in which the scalar order parameter is lower than $0.5S_b$, are indicated by the red surfaces as defects. (f) The colloidal potential energy in term of the center-center separation D in several fixed spatial arrangements, $\theta = 0°$, 20°, 45°, 70°, and 90°. (g) The log-log plots of the potential energies in (f). They are compared with the potential of hexadecapolar elastic distortion, $(D/R)^{-9}$. By fitting a power-law function $c(D/R)^{-\alpha}$ to the effective potentials, we get $\alpha = 9.31 \pm 0.28$, 8.97 ± 0.41, 9.06 ± 0.59, 8.76 ± 0.60, and 8.23 ± 0.49 for $\theta = 0°$, 20°, 45°, 70°, and 90°, respectively.

interactions, the director orientation and defect textures are studied at close contacts. We investigate the long-range interaction by interpolating it with a power law function.

Figure 5(a) shows that the particles undergo strong torques at the close contact separations. The effective potential energy explains that the colloidal particles can physically join together at $\theta \simeq 20^\circ$ or $\theta \simeq 70^\circ$ and form two independent colloidal arrangements with respect to the far director orientation. The effective potential height is so larger than the thermal energy k_BT that the equilibrium arrangements are spatially stable. They can form regular rhombic lattice of colloids when the particles confined to a two-dimensional page parallel to the director. In agreement with the experiment [9], we can decompose the whole particle surface into four attractive regions with different latitudes ($\theta \approx 20^\circ$, 70°, 110°, and 160°). We also show the director and the defect patterns around the particles in close contact interparticle arrangements as shown in Figs. 5(b)–5(e).

In Fig. 5(f), the effective potential obviously shows that the colloidal particles attract each other at $\theta = 20^\circ$ and 70° and repel each other at $\theta = 0^\circ$, $\theta = 45^\circ$, and 90°. In case of $\theta = 0^\circ$, the repulsive particle-particle interaction in the long distances turns to attractive in the short distances ($D/R \leqslant 2.2$). This behavior is due to the symmetry breaking of the director field. At the contact faces, the boojum defects are rearranged [see Fig. 5(b)]. Similar nonmonotonic interactions were observed in the colloids with the pure planar anchoring [6,17]. Around the particles with the normal anchoring, in the same way, we expected that the induced Saturn-ring defects rearrange at $\theta = 90^\circ$ and the close contact regimes, and this rearrangement of the defects gives rise to the bonding of the particles [7,14]. However, Fig. 5(e) shows that the closed surface disclination loops around the particles do not display such rearrangements in comparison with the Saturn-ring defects when the particles touch each other. Thus the short-range interactions between particles with the conical anchoring is more complex than those with the planar and normal anchorings.

To study the distance dependency of the colloidal interactions with conically anchoring at large separations, we compare the calculated effective colloidal potentials with those of two hexadecapolar moments at different spacial arrangements in Fig. 5(g) (see Appendix). It has been experimentally shown that the particle and the accompanying defects result in the anisotropic long-range interactions with the hexadecapole symmetry [9]. We fitted the effective potentials by the power function in all arrangements. Our results almost agree with the hexadecapolar elastic distortion as $\Delta F \propto (D/R)^{-9}$, although there remain some deviations between them.

V. SUMMARY

By modifying Nobili-Durand surface energy, we developed a surface energy in a form of the tensorial order parameter for describing the conically degenerate anchoring. It is compared with another surface energy, which was proposed by Sluckin and Poniewierski. We investigated the defect textures and the director orientations around a spherical colloid in the uniform nematic media by minimizing the Landau–de Gennes free energy with these surface energies at different equilibrium conic angles. Our calculations indicate that the local director orientation on the surface in the modified Nobili-Durand energy shows more adaptations with the expected equilibrium conic angle, in comparison to the Sluckin-Poniewierski surface energy.

Using the modified Nobili-Durand surface energy, we considered the interaction between two colloids with the equilibrium conic angle, $\psi_e = 45^\circ$. In agreement with experiments, the results show that there are two stable angular assemblies around $\theta \approx 20^\circ$ and 70° with respect to the far-field director orientation.

ACKNOWLEDGMENTS

Authors acknowledge discussions with Ivan I. Smalyukh, Tom C. Lubensky, and M. Reza Ejtehadi. S.R.S. acknowledges the partial financial supports from the Iran Ministry of Science, Research, and Technology. T.A. acknowledges the support from JSPS KAKENHI Grants No. JP25000002 and No. JP17K05612, and JST CREST Grant No. JPMJCR1424, Japan.

APPENDIX: INTERACTION BETWEEN POINT HEXADECAPOLES

We consider the interaction between the two colloids with the conically degenerated anchoring at large distances. At the large distance, the spherical colloid particle can be regarded as a point with the hexadecapole-moment density,

$$H^{ijkl}(\vec{r}) = H_0^{ijkl}[\delta(\vec{r}) + \delta(\vec{r} - \vec{D})], \tag{A1}$$

where H_0^{ijkl} is the magnitude of the moment density tensor.

The contribution of this moment to the free energy of the nematic liquid crystal host containing the particle is given by [20,39,40]

$$F_H = 4\pi K \int d\mathcal{V}[(\nabla \cdot \hat{n})(\hat{n} \cdot \nabla)^3 (H^{ijkl}\hat{n}_i\hat{n}_j\hat{n}_k\hat{n}_l)]. \tag{A2}$$

Assuming $\hat{n} = (\hat{n}_x, \hat{n}_y, 1)$, where $\hat{n}_x, \hat{n}_y \ll 1$, one obtain the total elastic free energy as

$$F_{\rm el} = K \int d\mathcal{V} \frac{1}{2}(\nabla \hat{n}_\mu)^2 + F_H. \tag{A3}$$

Its Euler-Lagrange equation is

$$\nabla^2 \hat{n}_\mu = -4\pi \partial_\mu \partial_z^3 H^{zzzz}. \tag{A4}$$

From Eqs (A1), (A3), and (A4), we obtain the mutual interaction energy between the colloids as

$$U(\vec{D}) = 4\pi K \frac{8! h_z^2}{|\vec{D}|^9} P_8(\cos\theta), \tag{A5}$$

where $h_z = H_0^{zzzz}$ and $P_8(x)$ is the eighth-order Legendre polynomial function of x.

[1] P. Poulin, H. Stark, T. C. Lubensky, and D. A. Weitz, Science **275**, 1770 (1997).

[2] I. Musevic, M. Skarabot, U. Tkalec, M. Ravnik, and S. Zumer, Science **313**, 954 (2006).

[3] C. P. Lapointe, T. G. Mason, and I. I. Smalyukh, Science **326**, 1083 (2009).

[4] J. Dontabhaktuni, M. Ravnik, and S. Zumer, Proc. Natl. Acad. Sci. USA **111**, 2464 (2014).

[5] S. M. Hashemi, U. Jagodic, M. R. Mozaffari, M. R. Ejtehadi, I. Musevic, and M. Ravnik, Nat. Commun. **8**, 14026 (2017).

[6] I. I. Smalyukh, O. D. Lavrentovich, A. N. Kuzmin, A. V. Kachynski, and P. N. Prasad, Phys. Rev. Lett. **95**, 157801 (2005).

[7] M. Ravnik, M. Škarabot, S. Žumer, U. Tkalec, I. Poberaj, D. Babič, N. Osterman, and I. Muševič, Phys. Rev. Lett. **99**, 247801 (2007).

[8] M. Conradi, M. Ravnik, M. Bele, M. Zorko, S. Zumer, and I. Musevic, Soft Matter **5**, 3905 (2009).

[9] B. Senyuk, O. Puls, O. M. Tovkach, S. B. Chernyshuk, and I. I. Smalyukh, Nat. Commun. **7**, 10659 (2016).

[10] B. Senyuk, J. Aplinc, M. Ravnik, and Ivan I. Smalyukh, arXiv:1811.03901v1 (2018).

[11] O. Guzman, E. B. Kim, S. Grollau, N. L. Abbott, and J. J. de Pablo, Phys. Rev. Lett. **91**, 235507 (2003).

[12] M. Yada, J. Yamamoto, and H. Yokoyama, Phys. Rev. Lett. **92**, 185501 (2004).

[13] J.-i. Fukuda, H. Stark, M. Yoneya, and H. Yokoyama, Phys. Rev. E **69**, 041706 (2004).

[14] T. Araki and H. Tanaka, Phys. Rev. Lett. **97**, 127801 (2006).

[15] J. Kotar, M. Vilfan, N. Osterman, D. Babic, M. Copic, and I. Poberaj, Phys. Rev. Lett. **96**, 207801 (2006).

[16] M. Vilfan, N. Osterman, M. Copic, M. Ravnik, S. Zumer, J. Kotar, D. Babic, and I. Poberaj, Phys. Rev. Lett. **101**, 237801 (2008).

[17] M. R. Mozaffari, M. Babadi, J. Fukuda, and M. R. Ejtehadi, Soft Matter **7**, 1107 (2011).

[18] P. Poulin and D. A. Weitz, Phys. Rev. E **57**, 626 (1998).

[19] R. W. Ruhwandl and E. M. Terentjev, Phys. Rev. E **55**, 2958 (1997).

[20] T. C. Lubensky, D. Pettey, N. Currier, and H. Stark, Phys. Rev. E **57**, 610 (1998).

[21] H. Stark, Phys. Rep. **351**, 387 (2001).

[22] M. Skarabot, M. Ravnik, S. Zumer, U. Tkalec, I. Poberaj, D. Babic, N. Osterman, and I. Musevic, Phys. Rev. E **77**, 031705 (2008).

[23] U. M. Ognysta, A. B. Nych, V. A. Uzunova, V. M. Pergamenschik, V. G. Nazarenko, M. Škarabot, and I. Muševič, Phys. Rev. E **83**, 041709 (2011).

[24] Z. Eskandari, N. M. Silvestre, M. Tasinkevych, and M. M. Telo da Gama, Soft Matter **8**, 10100 (2012).

[25] B. Senyuk, Q. Liu, E. Bililign, P. D. Nystrom, and I. I. Smalyukh, Phys. Rev. E **91**, 040501 (2015).

[26] S. R. Seyednejad, M. R. Mozaffari, T. Araki, and E. Nedaaee Oskoee, Phys. Rev. E **98**, 032701 (2018).

[27] S. M. Hashemi and M. R. Ejtehadi, Phys. Rev. E **91**, 012503 (2015).

[28] D. A. Beller, M. A. Gharbi, and I. B. Liu, Soft Matter **11**, 1078 (2015).

[29] A. Rapini and M. Papoular, J. Phys. Colloq. (France) **30**, C4-54 (1969).

[30] M. Nobili and G. Durand, Phys. Rev. A **46**, R6174 (1992).

[31] T. Sluckin and A. Poniewierski, *Fluid Interfacial Phenomena*, edited by C. A. Croxton (John Wiley, Chichester, 1986).

[32] O. O. Ramdane, P. Auroy, S. Forget, E. Raspaud, P. Martinot-Lagarde, and I. Dozov, Phys. Rev. Lett. **84**, 3871 (2000).

[33] J. B. Fournier and P. Galatola, Europhys. Lett. **72**, 403 (2005).

[34] V. Y. Rudyak, M. N. Krakhalev, V. S. Sutormin, O. O. Prishchepa, V. Y. Zyryanov, J.-H. Liu, A. V. Emelyanenko, and A. R. Khokhlov, Phys. Rev. E **96**, 052701 (2017).

[35] P. G. de Gennes and J. Prost, *The Physics of Liquid Crystal* (Oxford University Press, Oxford, 1995).

[36] S. Kralj, S. Zumer, and D. W. Allender, Phys. Rev. A **43**, 2943 (1991).

[37] C. Geuzaine and J.-F. Remacle, Int. J. Numer. Methods Eng. **79**, 1309 (2009).

[38] W. H. Press, S. A. Teukolsky, W. T. Vetterling, and B. P. Flannery, *Numerical Recipes*, 2nd ed. (Cambridge University Press, Cambridge, 1992).

[39] S. Ramaswamy, R. Nityananda, V. A. Raghunathan, and J. Prost, Mol. Cryst. Liq. Cryst. Sci. Technol. Sect. A **288**, 175 (1996).

[40] O. M. Tovkach, S. B. Chernyshuk, and B. I. Lev, Phys. Rev. E **86**, 061703 (2012).